JCSE Journal of Computing Science and Engineering

Invited Paper
Journal of Computing Science and Engineering,
Vol. 7, No. 2, June 2013, pp. 132-138

Brain Computer Interfacing: A Multi-Modal Perspective

Siamac Fazli* **and Seong-Whan Lee**
Department of Brain and Cognitive Engineering, Korea University, Seoul, Korea
fazli@korea.ac.kr, swlee@image.korea.ac.kr

Abstract
Multi-modal techniques have received increasing interest in the neuroscientific and brain computer interface (BCI) communities in recent times. Two aspects of multi-modal imaging for BCI will be reviewed. First, the use of recordings of multiple subjects to help find subject-independent BCI classifiers is considered. Then, multi-modal neuroimaging methods involving combined electroencephalogram and near-infrared spectroscopy measurements are discussed, which can help achieve enhanced and robust BCI performance.

Category: Human computing

Keywords: Brain computer interfaces; Multi-modal; Subject-independent classification; EEG-NIRS

I. INTRODUCTION

In recent brain computer interface (BCI) research, training and calibration times have been drastically reduced due to the use of machine learning and adaptive signal processing techniques [1] as well as novel dry electrodes [2-7]. Initial BCI systems were based on operant conditioning, and could easily require months of training on the subject side before it was possible to use them in an online feedback setting [8, 9].

Second-generation BCI systems required the recording of a brief calibration session, during which a subject assumes a fixed number of brain states such as that during movement imagination, after which subject-specific spatio-temporal filters [10] are inferred along with individualized classifiers [1]. The first steps to transfer a BCI user's filters and classifiers between sessions have been studied [11], and a further online study confirmed that such a transfer is indeed possible without significant performance loss [12]. However, while this work focused on reusing data from previous sessions of expert users, more recent approaches designed subject-independent zero-training BCI classifiers that enable both experienced and novice BCI subjects to use a BCI system immediately, without the need for recording calibration sessions [13-15]. Various of state-of-the-art learning methods (e.g., SVM, Lasso, etc.) have been applied in order to construct one-size-fits-all classifiers from a vast number of redundant features. The use of sparsifying techniques leads to features within the electroencephalogram (EEG) data that are predictive for future BCI users. The findings show a distribution of different alpha-band features in combination with a number of characteristic common spatial patterns (CSPs) that are highly predictive for most users. Clearly, these type of procedures may also be of use in scientific fields other than BCI, where complex characteristic features need to be homogenized into one overall inference model.

To date, EEG is the most widely used technology in the context of BCI. Some of the main reasons are the relatively low costs and fast setup times partly attributable to the advent of dry-electrode and subject-independent

Open Access http://dx.doi.org/10.5626/JCSE.2013.7.2.132 http://jcse.kiise.org

Received 3 May 2013, **Accepted** 8 May 2013
*Corresponding Author

Note that some of the results and figures have been published previously.

 pISSN: 1976-4677 eISSN: 2093-8020

classifiers. Another important reason is the high temporal resolution that EEG offers. However, EEG sensory motor rhythm (SMR)-based BCI still suffers from a number of problems. Unfortunately, not all subjects are able to alter their sensory motor rhythms, and thus, SMR-based BCIs do not work for all subjects. To this end, simultaneous recordings of near-infrared spectroscopy (NIRS) and EEG have not only been shown to increase BCI performance, but have also enabled some subjects to operate a BCI, who previously were not able to do so using solely EEG [16].

While EEG has the highest temporal resolution of all neuroimaging methods, NIRS is dependent on changes of blood flow, as it measures the oxygenated and deoxygenated hemoglobin (HbO_2 and HbR) in the superficial layers of the human cortex. The temporal resolution of NIRS is therefore orders of magnitudes lower, which substantially reduces the upper bound of information transfer rates (ITRs) for NIRS-based BCIs. Every neuroimaging method suffers from particular limitations. EEG has poor spatial resolution, while NIRS suffers from sluggishness of the underlying vascular response, which limits its temporal resolution. By employing a multi-modal neuroimaging approach, combining EEG and NIRS, it becomes possible to focus on their individual strengths and to partly overcome these limitations. In particular, we will review how extracting relevant NIRS features to support and complement high-speed EEG-based BCI and thus forming a *hybrid* BCI [17], allows for exploitation of the responsiveness of EEG (i.e., high ITR) as well as achieving enhanced and robust overall BCI performance by using information from the vascular response not contained within the EEG.

II. SUBJECT-INDEPENDENT BCI CLASSIFICATION

On the path of bringing BCI technology from the lab into practical use, it becomes indispensable to reduce the setup time. While dry electrodes provide a first step to eliminating the time needed for placing a cap, the need for recording calibration sessions has still remained. Employing a large body of high-quality experimental data accumulated over the years now enables the experimenter to choose, by means of machine learning technology, a very sparse set of voting classifiers, which perform as well as the standard, state-of-the-art subject-calibrated methods. L_1-regularized regression in this case performs better than other methods such as majority voting (Table 1). The features that show best generalization do not exclusively come from the best-performing subjects, and in fact, some average performers were also selected (Fig. 1). Interestingly, some subjects with very high BCI performance were not selected at all, while others generalized well in the sense that their models were able to predict other subjects' data. No single frequency band dominated with regard to classification accuracy (Fig. 1a). Therefore, diverse features must be selected for the regularization. Nevertheless, there is significant redundancy between classifiers in the ensemble. The approach of finding a sparse solution reduces the dimensionality of the chosen features significantly. For very able subjects, zero-training methods exhibit a slight performance decrease, though this will not prevent them from performing successfully in BCI. The sparsification of classifiers leads to insight into neurophysiological processes [15]. These processes identify relevant cortical locations and frequency bands of neuronal population activity that are in agreement with general neuroscientific knowledge. While these studies concentrated on zero-training classification and not brain activity interpretation, a much closer look is warranted. Movement imagination detection is not only determined by the cortical representation of the limb whose control is being imagined (in this case the arm), but also by differentially located cortical regions involved in movement planning (frontal), execution (fronto-parietal), and sensory feedback (occipito-parietal). Patterns relevant to BCI detection appear in all these areas, and while dominant discriminant frequencies are in the *a* range, higher frequencies appear in the ensemble, albeit in combination with less focused patterns. So, that which is found by the machine learning algorithm should be interpreted as representing the characteristic neurophysiological variation a large subject group, which in itself is a highly relevant topic.

III. MULTI-MODAL RECORDINGS FOR BCI

BCIs that solely rely on NIRS have been realized recently [18, 19]. However, when looking at plain NIRS classification rates, it becomes apparent that NIRS cannot be seen as a viable alternative to EEG-based BCIs on its own. However, in a combination with EEG, we find that NIRS is capable of significantly enhancing event-related desynchronization (ERD)-based BCI performance. Not only does it increase performance for most subjects, but it also allows for meaningful classification rates for those who would otherwise not be able to operate a solely EEG-based BCI [16].

Some subjects, who are able to operate SMR-based BCIs, experience a high level of non-stationarities in their BCI performance, as can be seen in Fig. 2. Possible solutions have been proposed, such as adaptive models [20, 21], stationary subspace analysis [22], and a multi-modal approach [23]. The findings indicate that the performance fluctuations of EEG-based BCI control can be predicted by the preceding NIRS activity. These NIRS-based predictions are then employed to generate new, more robust EEG-based BCI classifiers, which enhance classification significantly, while at the same time minimize performance fluctuations and thus increase the general stability

Table 1. Comparing subject-independent classifier result of various machine learning techniques to various baseline

Approach	Machine learning							Classical		
	Zero-training									Training
Method	Mean	kNN	LDA	LPM	SVM	LSR	LSR-ℓ_1	Lap	BP	CSP
# <25%	31	30	18	14	29	19	**36**	24	11	**39**
25%-tile	17.3	17.3	27.3	26.7	18.7	26.0	16.0	22.0	31.3	11.9
Median	30.7	31.3	36.0	37.3	**28.7**	36.7	**29.3**	34.7	38.7	**25.9**
75%-tile	41.3	42.0	43.3	44.0	41.3	44.0	40.7	45.3	45.3	41.4

kNN: k nearest neighbor, LDA: linear discriminant analysis, LPM: linear programming machine, SVM: support vector machine, LSR: least squares regression, Lap: Laplacian, BP: band power, CSP: common spatial pattern.

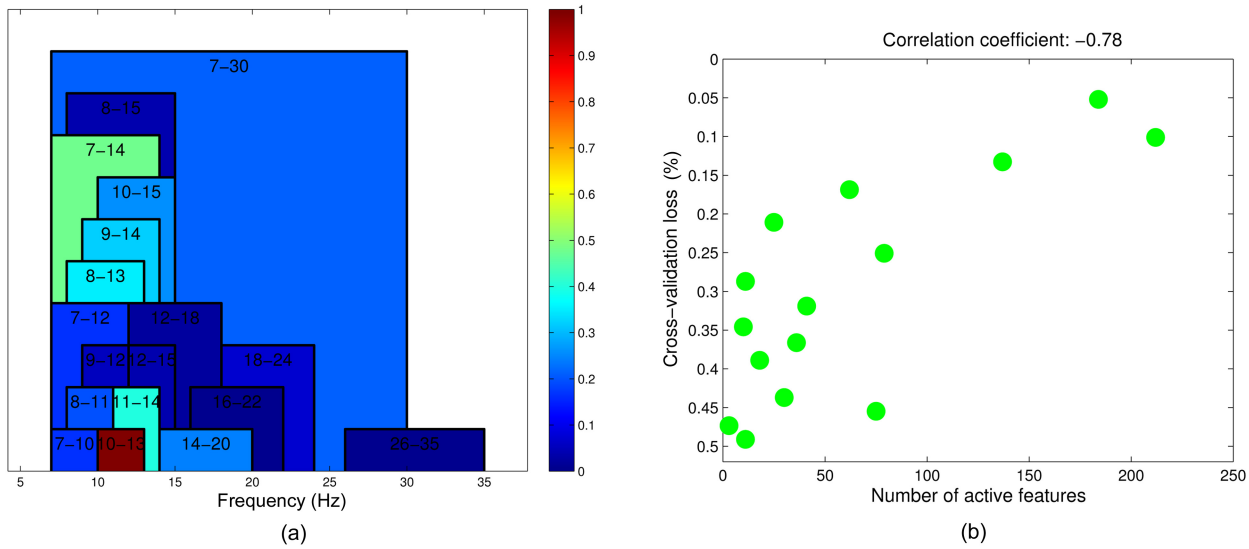

Fig. 1. (a) The used temporal filters and in color-code their contribution to the final L_1-regularized regression classification (the scale is normalized from 0 to 1). Cleary μ-band temporal filters between 10-13 Hz are most predictive. (b) Number of features used vs. self-predicted cross-validation. A high self-prediction can be seen to yield a large number of features that are predictable for the whole ensemble.

of BCI performance [23].

Two blocks of real-time EEG-based, visual feedback-controlled motor imagery (50 trials per block per condition) were recorded for the estimation of the EEG classifier. The first 2 seconds of each trial began with a black fixation cross, which appeared at the center of the screen. Then, an arrow appeared as a visual cue pointing to the left or right, and the fixation cross started moving for 4 seconds, according to the classifier output. After 4 seconds, the cross disappeared and the screen remained blank for 10.5 ± 1.5 seconds. The online processing was based on the concept of *coadaptive calibration* [21].

The user was given instantaneous EEG-based BCI feedback for the two blocks of motor imagery. During the first block of 100 trials, a subject-independent classifier was used, depending on band power estimates of Laplacian-filtered, motor-related EEG channels. For the second block subject-dependent spatial and temporal filters were estimated from the data of the first block and combined with some subject-independent features to form the classifier for the second block. During the online feedback, features were calculated every 40 ms with a sliding window of 750 ms. For further details on *coadaptive calibration,* we would like to refer the reader to a study by Vidaurre et al. [21].

Once the EEG classifier is estimated, a feedback block with 300 trials and a relatively short inter-stimulus interval of 7 seconds is recorded, lasting a total of 35 minutes. As before, the first 2 seconds of each trial began with the appearance of a black fixation cross at the center of the screen. Then, a visual cue in the form of an arrow appeared to indicate the required class, and the fixation cross started moving for 4 seconds, according to the classifier output. After the 4 seconds, the cross disappeared

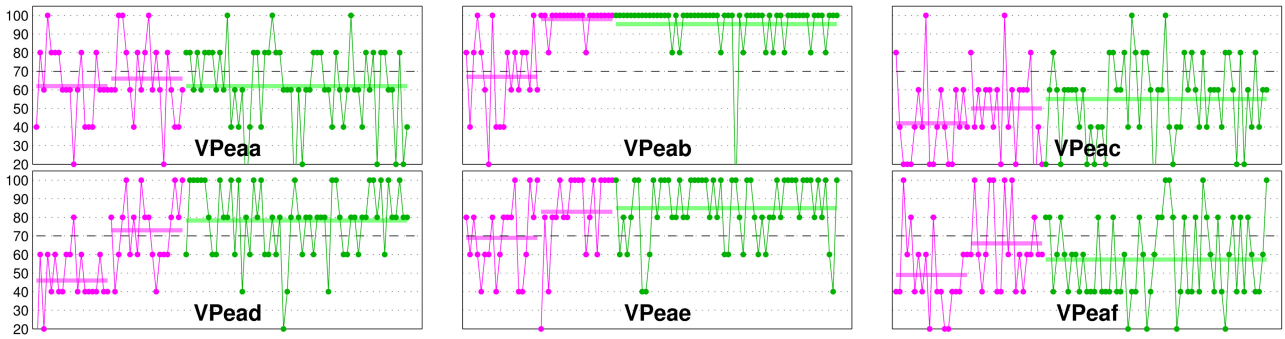

Fig. 2. The electroencephalogram classification rate is generally non-stationary in time. We show the fluctuations in performance for the first 6 subjects. Each dot represents the classification performance of 5 trials. On the y-axis the classification accuracy is depicted in percent, and the x-axis represents the time-course of the experiment. The magenta color shows early stages of the experiment, where the classifier is not yet considered to be stable, the green indicates a later state of the experiment, where the classifier is kept constant. Horizontal lines show the average classification performance.

and the screen remained blank for a short interval of 1 ± 0.5 seconds before the next trial began.

The long inter-trial intervals in the first two blocks were chosen to evaluate the NIRS signals with respect to motor imagery [16]. Here, we only investigate the 300 trials of the fast feedback dataset. These trials are split into chronological blocks of 5 trials each, resulting in 60 blocks and the EEG-BCI performance of these smaller blocks are computed. For each block the EEG-based classifier output, *out* is multiplied by its true label $\tilde{y}$ and summed over the 5 trials within the block, resulting in the performance y of the given block:

$$y_k = \sum_{i=1}^{5} \tilde{y}_i \cdot \mathrm{out}_i \,, \tag{1}$$

where i is the trial within block k. By calculating the performance this way, a continuous performance measure can be obtained, which is preferable to a mere 0–1 loss, since it is more accurate and also more suitable for the purpose of regressing NIRS features onto this measure, which will be explained. The overall performance is subtracted from each block-performance, such that a 'time course' of above- and below-average EEG-BCI performance is obtained.

The NIRS signal is divided into multiple epochs, each with a width of 2 seconds, preceding each 5-trial block by 2, 4, 6, 8, and 10 seconds. Noisy channels are discarded, and the signal is transferred into the spectral domain. An L_1-regularized regression optimization problem [24] is formulated (and implemented with CVX [25]) to identify spectral NIRS features predicting the EEG performance of the following 5 trials:

$$\underset{\beta}{\operatorname{argmin}} \; \|y - \beta X\|_2 + \lambda \|\beta\|_1 \tag{2}$$

where X are the preceding NIRS features, β is the regressor, and λ is the regularization variable. Refer to Fig. 3 for a graphical explanation. The thin black boxes on the

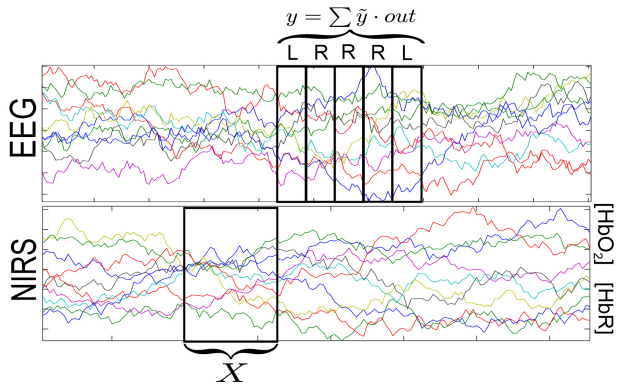

Fig. 3. The continuous electroencephalogram (EEG) during the fast feedback phase (top). The simultaneously recorded continuous oxygenated and deoxygenated hemoglobin (HbO_2 and HbR) near-infrared spectroscopy (NIRS) chormophores. Note that random data is shown here for visualization purposes (bottom).

upper part represent trials, where left and right-hand motor imagery are cued. The optimization problem is repeated 60 times, and each time a different block is left out, resulting in a performance prediction for each block. Using the predictions as well as the actual performance, the correlation coefficient and its p-value are calculated. The corresponding p-values test the hypothesis of zero correlation. Since the method is repeated a number of times for various intervals, the p-values are Bonferroni corrected.

Depending on the prediction of the NIRS, the EEG data is grouped into three categories: blocks with good performance, medium performance, and bad performance. All three groups have an even number of trials (100 trials per group). A validation scheme is setup, where one block (consisting of 5 trials) is left out as a test-set. Using the training, set we calculate four EEG classifiers: one for each group, defined by the performance prediction, and a fourth comprising all training data. The individual classi-

Table 2. Correlation coefficients (cc) and p-values (p) of predicted vs. actual electroencephalogram performances

Subject	an	ab	ae	aj	af	ah	am	ai	ad	ag	aa	ak	al	ac
cc	0.66	0.56	0.54	0.49	0.48	0.48	0.44	0.43	0.41	0.37	0.36	0.35	0.32	0.18
p	5.3e-07	1.5e-04	3.0e-04	0.003	0.004	0.004	0.016	0.020	0.040	0.135	0.162	0.235	0.550	6.523

Table 3. Percentage classification loss of all individual subjects as well as their means

Subject	All	Meta	Good	Medium	Bad
ae	18.7	20.3	25.0	19.3	24.3
aj	10.7	8.7	14.3	14.7	22.7
ah	4.3	4.0	5.0	15.3	6.0
an	3.7	3.3	2.7	3.0	3.7
ai	21.0	11.7	20.0	12.0	25.0
al	12.3	14.7	20.3	16.0	27.0
af	48.0	44.3	49.7	48.0	44.0
aa	42.7	41.0	41.7	45.0	45.7
ag	29.3	21.7	24.0	35.7	35.7
ad	24.0	20.3	21.3	21.7	31.0
ak	14.7	11.0	33.0	15.7	16.0
am	46.0	38.0	41.7	41.7	41.0
ac	35.7	33.7	38.0	37.3	41.0
ab	13.0	13.0	14.0	12.7	14.0
Mean	23.1	**20.4***	25.0	24.1	26.9

all stands for the standard procedure, where all training trials are considered the same; *good* uses only training trials from blocks with good performance; *medium* uses trials with average performance; *bad* trials uses trials with low performance, and *meta* stands for a meta-classifier, which combines classifiers of *all*, *good*, *medium* and *bad*.

fiers consist of a fixed broadband temporal filter (5th-order Butterworth digital filter with 5–30 Hz), a spatial filter (CSP [10]) and a linear classifier (LDA). In a second step, we train a meta-classifier, combining all four individual classifiers, based on the training set. The outputs of this meta-classifier are then compared to the true labels of the left-out trials, and its 0–1 loss is computed. This procedure is repeated for all blocks. As a baseline, we use the EEG classifier that was trained on all training data.

Table 2 shows the results of the optimization problem defined by Equation (2). For 9 out of 14 subjects, the p-values of the correlation coefficients calculated between the predicted and actual EEG performance are significant.

Table 3 shows the classification results of all subjects, and their means. A paired t-test between the standard procedure of treating all training trials the same, as compared to a meta-classifier that combines four classifiers, based on the performance of blocks, results in a value of

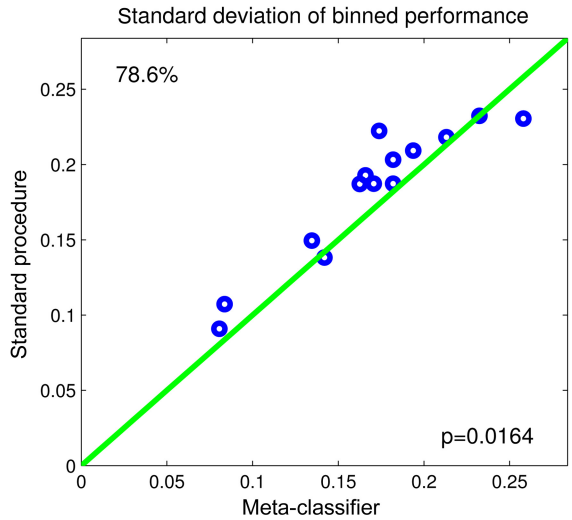

Fig. 4. Scatter-plot of the standard deviation of performance over all blocks. Each dot represents a single subject. The percentage on the top left indicates for how many subjects the meta classifier has lower standard deviation. p indicated the significance of a paired t-test.

p = 0.013 (which is indicated by a '*' in Table 3).

To evaluate whether our method reduces the performance variability during the feedback session, we calculate the standard deviation over all 60 blocks for the standard method, where all trials are treated the same, as well as for the meta-classifier.

Fig. 4 shows the results in the form of a scatter-plot. As can be seen, our proposed method reduces the variability of performance in 11 out of 14 subjects. In one subject, the variability is the same, and for two subjects, the standard procedure has lower performance fluctuations. A paired t-test reveals a significant relationship with $p < 0.05$.

IV. DISCUSSION

Multi-modal techniques can be useful in a number of ways. For the case of subject-independent decoding, we found that the outcome of a machine learning experiment can also be viewed as a compact quantitative description of the characteristic variability between individuals in the large subject group. Note that it is not the best subjects that characterize the variance necessary for a subject-independent algorithm, but the spread over existing physiology is represented concisely.

For the case of combining NIRS and EEG, it can be concluded that this novel approach of combining NIRS and EEG is a viable technique, suitable for SMR-based BCI, since it preserves the responsiveness of the EEG, while at the same time significantly enhances classification rates, and minimizes performance fluctuations.

REFERENCES

1. G. Dornhege, J. R. Millan, T. Hinterberger, D. McFarland, and K. R. Muller, *Toward Brain-Computer Interfacing*, Cambridge, MA: MIT Press, 2007.
2. F. Popescu, S. Fazli, Y. Badower, B. Blankertz, and K. R. Muller, "Single trial classification of motor imagination using 6 dry EEG electrodes," *PLoS ONE*, vol. 2, no. 7, p. e637, 2007.
3. C. Grozea, C. D. Voinescu, and S. Fazli, "Bristle-sensors: low-cost flexible passive dry EEG electrodes for neurofeedback and BCI applications," *Journal of Neural Engineering*, vol. 8, no. 2, p. 25008, 2011.
4. T. O. Zander, M. Lehne, K. Ihme, S. Jatzev, J. Correia, C. Kothe, B. Picht, and F. Nijboer, "A dry EEG-system for scientific research and brain-computer interfaces," *Frontiers in Neuroscience*, vol. 5, p. 53, 2011.
5. Y. M. Chi, Y. T. Wang, Y. Wang, C. Maier, T. P. Jung, and G. Cauwenberghs, "Dry and noncontact EEG sensors for mobile brain-computer interfaces," *IEEE Transactions on Neural Systems and Rehabilitation Engineering*, vol. 20, no. 2, pp. 228-235, 2012.
6. L. D. Liao, C. Y. Chen, I. J. Wang, S. F. Chen, S. Y. Li, B. W. Chen, J. Y. Chang, and C. T. Lin, "Gaming control using a wearable and wireless EEG-based brain-computer interface device with novel dry foam-based sensors," *Journal of Neuroengineering and Rehabilitation*, vol. 9, no. 1, p. 5, 2012.
7. C. Guger, G. Krausz, B. Z. Allison, and G. Edlinger, "Comparison of dry and gel based electrodes for P300 brain-computer interfaces," *Frontiers in Neuroscience*, vol. 6, p. 60, 2012.
8. T. Elbert, B. Rockstroh, W. Lutzenberger, and N. Birbaumer, "Biofeedback of slow cortical potentials. I," *Electroencephalography and Clinical Neurophysiology*, vol. 48, no. 3, pp. 293-301, 1980.
9. N. Birbaumer, N. Ghanayim, T. Hinterberger, I. Iversen, B. Kotchoubey, A. Kubler, J. Perelmouter, E. Taub, and H. Flor, "A spelling device for the paralysed," *Nature*, vol. 398, no. 6725, pp. 297-298, 1999.
10. B. Blankertz, R. Tomioka, S. Lemm, M. Kawanabe, and K. R. Muller, "Optimizing spatial filters for robust EEG single-trial analysis," *IEEE Signal Processing Magazine*, vol. 25, no. 1, pp. 41-56, 2008.
11. M. Krauledat, M. Schroder, B. Blankertz, and K. R. Muller, "Reducing calibration time for brain-computer interfaces: a clustering approach," in *Advances in Neural Information Processing Systems 19*, B. Scholkopf, J. Platt, and T. Hoffman, editors, Cambridge, MA: MIT Press, 2007, pp. 753-760.
12. M. Krauledat, M. Tangermann, B. Blankertz, and K. R. Muller, "Towards zero training for brain-computer interfacing," *PLoS ONE*, vol. 3, no. 8, p. e2967, 2008.
13. S. Fazli, F. Popescu, M. Danoczy, B. Blankertz, K. R. Muller, and C. Grozea, "Subject-independent mental state classification in single trials," *Neural Networks*, vol. 22, no. 9, pp. 1305-1312, 2009.
14. S. Fazli, C. Grozea, M. Danoczy, B. Blankertz, F. Popescu, and K. R. Muller, "Subject independent EEG-based BCI decoding," in *Advances in Neural Information Processing Systems 22*, Y. Bengio, D. Schuurmans, J. Lafferty, C. K. I. Williams, and A. Culotta, editors, North Miami Beach, FL: Curran Associates, 2009, pp. 513-521.
15. S. Fazli, M. Danoczy, J. Schelldorfer, and K. R. Muller, "(1)-penalized linear mixed-effects models for high dimensional data with application to BCI," *Neuroimage*, vol. 56, no. 4, pp. 2100-2108, 2011.
16. S. Fazli, J. Mehnert, J. Steinbrink, G. Curio, A. Villringer, K. R. Muller, and B. Blankertz, "Enhanced performance by a hybrid NIRS-EEG brain computer interface," *Neuroimage*, vol. 59, no. 1, pp. 519-529, 2012.
17. G. Pfurtscheller, B. Z. Allison, C. Brunner, G. Bauernfeind, T. Solis-Escalante, R. Scherer, T. O. Zander, G. Mueller-Putz, C. Neuper, and N. Birbaumer, "The hybrid BCI," *Frontiers in Neuroscience*, vol. 4, p. 30, 2010.
18. T. Tsubone, T. Muroga, and Y. Wada, "Application to robot control using brain function measurement by near-infrared spectroscopy," in *Proceedings of the 29th Annual International Conference of the IEEE Engineering in Medicine and Biology Society*, Lyon, France, 2007, pp. 5342-5345.
19. A. F. Abdelnour and T. Huppert, "Real-time imaging of human brain function by near-infrared spectroscopy using an adaptive general linear model," *Neuroimage*, vol. 46, no. 1, pp. 133-143, 2009.
20. M. Krauledat, "Analysis of nonstationarities in EEG signals for improving brain-computer interface performance," Ph.D. dissertation, Fakultat IV Elektrotechnik und Informatik, Technische Universität Berlin, Berlin, Germany, 2008.
21. C. Vidaurre, C. Sannelli, K. R. Muller, and B. Blankertz, "Co-adaptive calibration to improve BCI efficiency," *Journal of Neural Engineering*, vol. 8, no. 2, p. 25009, 2011.
22. P. von Bunau, F. C. Meinecke, F. Kiraly, and K. R. Muller, "Finding stationary subspaces in multivariate time series," *Physical Review Letters*, vol. 103, no. 21, p. 214101, 2009.
23. S. Fazli, J. Mehnert, J. Steinbrink, and B. Blankertz, "Using NIRS as a predictor for EEG-based BCI performance," in *Proceedings of the 34th Annual International Conference of the IEEE Engineering in Medicine and Biology Society*, San Diego, CA, 2012, pp. 4911-4914.
24. R. Tibshirani, "Regression shrinkage and selection via the Lasso," *Journal of the Royal Statistical Society B*, vol. 58, no. 1, pp. 267-288, 1996.
25. M. Grant and S. Boyd, "CVX: MATLAB software for disciplined convex programming, version 1.21," http://cvxr.com/cvx, April 2011.

Siamac Fazli

Siamac Fazli received his B.Sc. Physics degree from the University of Exeter in 2002, his M.Sc. in Medical Neuroscience from the Humboldt University Berlin in 2004 and in 2011 he finished his Ph.D. at the Berlin Institute of Technology under the supervision of Prof. Dr. Klaus-Robert Müller. He worked as a Postdoctoral Researcher at the Berlin Institute of Technology within the Departments of Neurotechnology and Machine Learning. In particular he was involved in the Bernstein Focus: Neurotechnology (BFNT) project and part of the Berlin Brain-Computer Interface (BBCI) group. Recently, he has been appointed as an Assistant Professor at Korea University within the Department of Brain and Cognitive Engineering. His main research interests include Brain-Computer Interfaces, machine learning, multi-modal neuroimaging and neuroscience.

Seong-Whan Lee

Seong-Whan Lee is the Hyundai-Kia Motor Chair Professor at Korea University, where he is the head of the Department of Brain and Cognitive Engineering and the director of the Institute for Brain and Cognitive Engineering.

He received the B.S. degree in computer science and statistics from Seoul National University, Seoul, Korea, in 1984, and the M.S. and Ph.D. degrees in computer science from Korea Advanced Institute of Science and Technology in 1986 and 1989, respectively.

From February 1989 to February 1995, he was an Assistant Professor in the Department of Computer Science at Chungbuk National University, Cheongju, Korea. In March 1995, he joined the faculty of the Department of Computer Science and Engineering at Korea University, Seoul, Korea, and now he is the tenured full professor. In 2001, he stayed at the Department of Brain and Cognitive Sciences, MIT as a visiting professor.

A Fellow of the IEEE, IAPR, and Korean Academy of Science and Technology, he has served several professional societies as chairman or governing board member. He was the founding Co-Editor-in-Chief of the International Journal of Document Analysis and Recognition and has been an Associate Editor of several international journals: Pattern Recognition, ACM Trans. on Applied Perception, IEEE Trans. on Affective Computing, Image and Vision Computing, International Journal of Pattern Recognition and Artificial Intelligence, and International Journal of Image and Graphics.

His research interests include pattern recognition, computer vision, and brain engineering. He has more than 250 publications in international journals and conference proceedings, and authored 10 books.